Martensite Transformation and Magnetic Properties of Ni-Fe-Ga Heusler Alloys

HRUSIKESH NATH and GANDHAM PHANIKUMAR

Compositional instability and phase formation in Ni-Fe-Ga Heusler alloys are investigated. The alloys are synthesized into two-phase microstructure. Their structures are identified as fcc and L_{21}, respectively. The γ-phase formation could be suppressed with higher Ga-content in the alloy as Ga stabilizes austenite phase, but Ga lowers the martensite transformation temperature. The increase of Fe content improves the magnetization value and the increase of Ni from 52 to 55 at. pct raises the martensite transformation temperature from 216 K to 357 K (−57 °C to 84 °C). Magnetic properties and martensitic transformation behavior in Ni-Fe-Ga Heusler alloys follow opposite trends, while Ni replaces either Fe or Ga, whereas they follow similar trends, while Fe replaces Ga. Modulated martensite structure has low twinning stress and high magneto crystalline anisotropic properties. Thus, the observation of 10- and 14 M-modulated martensite structures in the studied Ni-Fe-Ga Heusler alloys is beneficial for shape memory applications. The interdependency of alloy composition, phase formation, magnetic properties, and martensite transformation are discussed.

DOI: 10.1007/s11661-015-3098-7

I. INTRODUCTION

FERROMAGNETIC Heusler alloys are a new class of materials which exhibit large magnetoelastic strain and magnetocaloric effect due to the structural transition. Ni-Mn-Ga Heusler alloys show large magnetic field-induced strain. However, the fragile nature of Ni-Mn-Ga alloy creates scope for the development of other Heusler systems with improved mechanical properties. Several other Ni-based Heusler alloys such as Ni-Mn-In, Ni-Mn-Sn, Ni-Mn-Sb also show magnetostructural transition.[1–3] Ni-Fe-Ga Heusler alloy seems to have potential ability to replace Ni-Mn-Ga. The ductility Ni-Fe-Ga Heusler alloy is improved by the induction of γ-phase in the microstructure along with the presence of austenite phase.[4,5] Ni-Fe-Ga Heusler alloys also exhibit 10, 14 M martensite microstructures and is a strong contender for magnetic shape memory applications.[5–10] Martensite transformation in Heusler alloys proceeds dynamically and more often associated with structural modulation in martensite phase.[11] Atoms vibrate and deviate from their static equilibrium lattice positions in such a way that the modulated wave propagates through the lattice with certain periodicity. 10 and 14 M represents the corresponding periodicity of the lattice modulation of the martensite phase. For 10 or 14 M, the vibration has the periodicity of 10 or 14 atomic positions, respectively. In such cases, the tetragonal symmetry of martensite phase no longer exists and has orthorhombic or monoclinic symmetry due to crystal modulation. The detailed crystal modulations of martensite phase in Heusler alloys are described elsewhere.[6,7] Thorough investigation on phase-formation behavior in Ni-Fe-Ga Heusler alloy and their compositional dependency would definitely improve the understanding of the interaction of structural and magnetic states leading to magnetostructural transition.

In the earlier work, it was concluded that γ-phase and austenite form competitively and phase separation takes place because of their variation in Fe/Ga content.[12] In this paper we discuss the dynamics of phase formation in Ni-Fe-Ga Heusler alloys, their structural properties, the effect of alloy composition on magnetic properties, and martensite transformation behavior. Phase evolution in Ni-Fe-Ga Heusler alloys is relatively complex and not well studied. Studies on phase and microstructural evolution in Ni-Fe-Ga Heusler alloys, their structural and magnetic properties, phase transitions, and related phenomena are important to bring this alloy toward the intended shape memory applications.

II. MATERIALS AND METHODS

Nine different ternary Ni-Fe-Ga Heusler alloys were prepared by varying the alloy composition around Heusler stoichiometry X_2YZ ($Ni_{50}Fe_{25}Ga_{25}$). They form three different series of alloys, namely $Ni_{52+x}Fe_{22-x}Ga_{26}$, $Ni_{52+y}Fe_{20}Ga_{28-y}$ and $Ni_{52}Fe_{19+z}Ga_{29-z}$ ($x\ y\ z = 0\ 1\ 2\ 3$) (Figure 1). As the total number of alloys are divided into three groups, few of them are common such as alloy $x = 0$ is same as alloy $z = 3$, alloy $x = 2$ is same as alloy $y = 2$ and alloy $y = 0$ is same as alloy $z = 1$. The different series of alloys, and

HRUSIKESH NATH, Research Scientist, and GANDHAM PHANIKUMAR, Associate Professor, are with the Department of Metallurgical and Materials Engineering, Indian Institute of Technology (IIT) Madras, Chennai 600036, India. Contact e-mail: hrushikesh.nath@gmail.com
Manuscript submitted June 2, 2015.
Article published online August 26, 2015

their magnetic and martensitic transformation properties are listed in Table I. Alloys were prepared by arc melting process in argon atmosphere in order to prevent oxidation of the alloys during the synthesis. Once the alloy buttons are prepared, they were annealed at 1273 K (1000 °C) for 1 hour each separately by sealing inside an evacuated quartz tube (10^{-5} mbar). They were quenched in water along with the quartz tube. This heat-treatment process enables the homogenization of the alloy composition and improves the structural ordering.

X-ray diffraction was used as the primary technique for structural characterization by X'Pert PANalytical using Cu-Kα radiation. The Heusler alloy samples were scanned in the 2θ ranging from 20 to 120 deg with 0.02 step size. Alloy compositions were analyzed using energy dispersive X-ray spectroscopic technique (EDX) attached with SEM without etching the samples to avoid any compositional loss from the surface. The nominal compositions are given in Table I. Some of the alloys are good to capture SEM images in backscattered electron imaging mode as they are having two-phase microstructures with the compositional differences across the phase boundary. However, the single-phase polycrystalline samples need to be etched in order to get the image in SEM. It is also difficult to observe the martensitic morphologies without etching the sample having martensitic structure. The etchant used for this purpose in Ni-Fe-Ga Heusler alloys is 10 pct nital for duration ranging from 60 to 300 seconds by swabbing technique. Sample preparation for TEM analysis is vital to get the desired or expected microstructural properties. Therefore, utmost care has been taken to prepare the TEM samples using Gatan ion miller (Model 691). Both the jets of the ion guns were kept at higher angle of 8 deg initially, and slowly the angle was brought down up to 4 deg as the sample gets thinned down by observing constantly. Structural phase transition was studied using differential scanning calorimetry (DSC) at heating/cooling rate of 10 K/min (10 °C/min) in the temperature range from 148 K to 373 K (−125 °C to +100 °C). Room-temperature magnetic properties of all the Ni-Fe-Ga Heusler alloys were studied using variable sample magnetometer (VSM, Lakeshore 2000). Initially degaussing procedure was followed, and VSM was calibrated with Ni-standard sample for magnetic moment measurement.

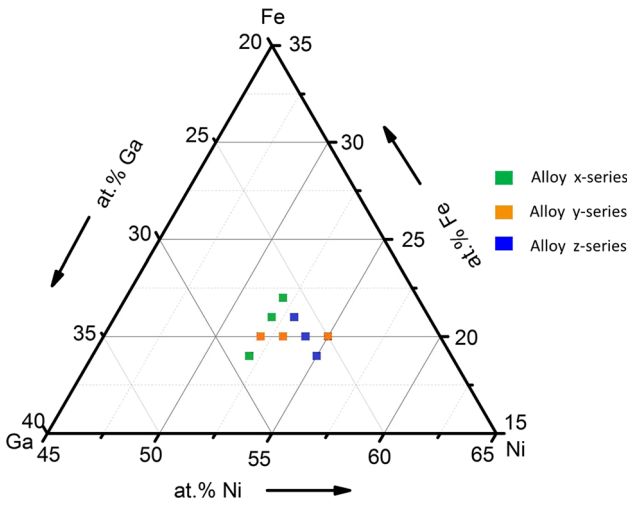

Fig. 1—A schematic of Ni-Fe-Ga system showing the alloys studied (alloy series x, y, z) in this article; phase identification is given in Table I.

III. RESULTS

A. *Microstructural Characterization*

The crystal structures of different phases present in all the Ni-Fe-Ga alloys are analyzed using X-ray diffraction and presented in Figures 2(a) through (c). The two-phase microstructures of alloys $x = 0, 1, 2$ correspond to γ-phase and austenite, with their structures being fcc and L_{21}, respectively (Figure 2). Modulated martensite structure is indentified in alloy $x = 3$ along with the presence of γ-phase. The appearance of four extra peaks around the main diffracted intense peak (220) at 2θ of approximately 44 deg is due to the 10 M structural modulation. In alloy $x = 3$, the presence of martensite phase in the microstructure along with γ-phase could be attributed to higher Ni-content (55 at. pct). The Increase in Ni-content in the alloy raises the structural transition temperature so that austenite transforms to martensite above room temperature.

In the case of alloys $y = 1, 2$, the two-phase microstructures of γ-phase and austenite are observed. Alloy $y = 3$ has martensite structure which is identified to be 14 M-modulated structure as observed from XRD patterns and confirmed in TEM studies. Similar type of splitting of XRD peak was reported by Li *et al.*[13] as 14 M crystal modulation in martensite being observed in Ni-Fe-Ga Heusler alloys.

Alloys $z = 0, 1$ form single-phase austenite microstructure having L_{21}-ordered structure (Figure 2(c)). This can be attributed to higher Ga content in both the alloys more than 27 at. pct. Higher amount of Ga content replacing Fe in the alloy tends to stabilize more of austenite than γ-phase. It has been reported elsewhere that single-phase austenitic microstructure forms in off-stoichiometric Ni-Fe-Ga Heusler alloys with Ga replacing Fe by more than 27 at. pct.[14] Lattice parameter of L_{21} structure of austenite phase in alloy $z = 0$ (0.5757 nm) is greater than that of in alloy $z = 1$ (0.5745 nm). The increase in lattice size could be attributed to higher amount of Ga content in alloy $z = 0$. While Ga replaces Fe in the alloy composition, it expands the lattice (as the atomic size of Ga is larger than Fe). For alloys $z = 2$ and 3, both γ-phase and austenite are observed in the microstructure as Ni is 52 at. pct in the alloy composition.

The parallel lath-like morphologies of martensite in alloy $x = 3$ are shown in Figure 3. The other phase in the microstructure is γ-phase, having dendritic morphology. The γ-phase happens to be the primary phase, nucleates, and grows first during solidification. Martensite twin bands are very much localized inside the martensite strips spread across the microstructure. That

Table I. Phases Present Along with the Compositions, Magnetic Properties, and Martensitic Transformation Temperatures of the Ni-Fe-Ga Heusler Alloys Studied

Composition	Phases Present	T_m [K (°C)]	M	e/a ratio
$Ni_{52+x}Fe_{22-x}Ga_{26}$ Heusler alloys				
$Ni_{52}Fe_{22}Ga_{26}$	aus and γ-phase	259 (−14)	36.36	7.74
$Ni_{53}Fe_{21}Ga_{26}$	aus and γ-phase	271 (−2)	22.71	7.76
$Ni_{54}Fe_{20}Ga_{26}$	aus and γ-phase	283 (10)	20.87	7.78
$Ni_{55}Fe_{19}Ga_{26}$	mart and γ-phase	345 (72)	16.79	7.80
$Ni_{52+y}Fe_{20}Ga_{28-y}$ Heusler alloys				
$Ni_{52}Fe_{20}Ga_{28}$	austenite	242 (−31)	28.0	7.64
$Ni_{53}Fe_{20}Ga_{27}$	aus and γ-phase	254 (−19)	25.71	7.71
$Ni_{54}Fe_{20}Ga_{26}$	aus and γ-phase	283 (10)	20.87	7.78
$Ni_{55}Fe_{20}Ga_{25}$	mart and γ-phase	357 (84)	11.43	7.85
$Ni_{52}Fe_{19+z}Ga_{29-z}$ Heusler alloys				
$Ni_{52}Fe_{19}Ga_{29}$	austenite	216 (−57)	15.07	7.59
$Ni_{52}Fe_{20}Ga_{28}$	austenite	242 (−31)	28.0	7.64
$Ni_{52}Fe_{21}Ga_{27}$	aus and γ-phase	250 (−23)	34.98	7.69
$Ni_{52}Fe_{22}Ga_{26}$	aus and γ-phase	259 (−14)	36.36	7.74

All the elemental compositions are given in at. pct taken from SEM-EDX analysis. aus = austenite and mart = martensite, martensite transformation temperature (T_m) in Kelvin (K) and in degree Celsius (°C), room-temperature magnetization (M) is in emu/g, e/a ratio represents the ratio of valence electrons to the number of atoms in the stoichiometry of the corresponding Heusler alloy.

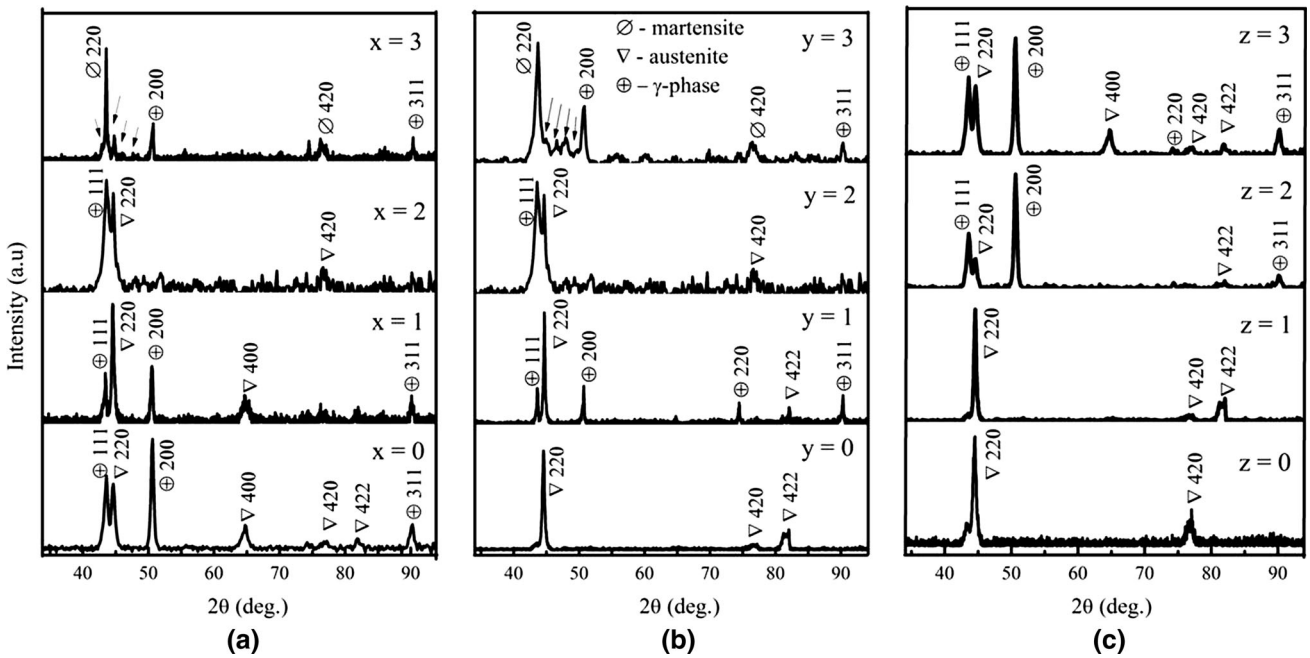

Fig. 2—X-ray diffraction patterns of (*a*) $Ni_{52+x}Fe_{22-x}Ga_{26}$, (*b*) $Ni_{52+y}Fe_{20}Ga_{28-y}$, (*c*) $Ni_{52}Fe_{19+z}Ga_{29-z}$ Heusler alloys showing the presence of γ-phase, austenite, and martensite in alloys marked accordingly.

can be the mixture of lath- and plate-like morphologies. The FEG-SEM images in Figure 3 show enlarged views of various morphologies of martensite present in the microstructure. Twinned parallel plates of martensite along with twin bands and martensite laths are shown in Figures 3(a), (b), and (d). Another *zig–zag* butterfly-like morphology could be seen from Figure 3(c). Different martensite morphologies including the butterfly-like morphology are discussed by Umemoto *et al.*[15] The formation of different types of morphologies in the alloy presents a composite microstructure and has strong influence on its mechanical and functional properties. The presence of γ-phase once again improves the composite nature of microstructure and adds up to the derived properties.

B. *Electron Diffraction and Imaging*

TEM images of single-phase austenite microstructure of alloys $z = 0$ and 1 are shown in Figures 4(a) and (b), respectively. The presence of (−12−1) (marked in arrows in Figure 4(a), inset) supper lattice reflections in the diffraction pattern of alloy $z = 0$ confirms the L_{21} ordering of austenite. The striations appear in the

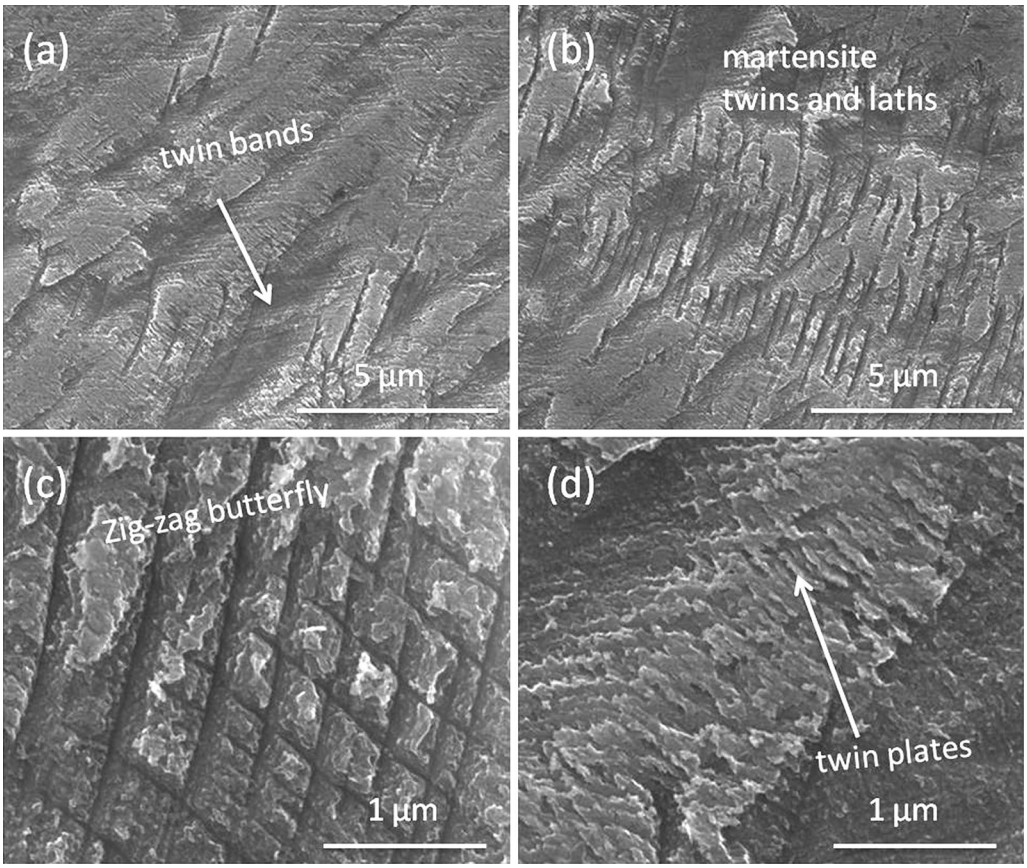

Fig. 3—Different morphologies of martensite such as twins, plates, butterfly are shown in (*a* through *d*) FEG-SEM images of alloy $x = 3$.

diffraction pattern (Figures 4(b), inset) is due the presence of tweed contrast in the microstructure of alloy $z = 1$ (Figure 4(b)). TEM images of alloy $x = 1$ exhibiting the presence of γ-phase and tweed contrast in austenite phase are shown in Figure 4(c) along with the phase interface. The indexed diffraction pattern of γ-phase is shown in the inset. The enlarged view of tweed contrast in alloy $x = 1$ is shown in Figure 4(d). The diffraction pattern and tweed contrast in alloy $x = 2$ are shown in Figures 4(e) and (f), respectively. The TEM diffraction patterns studied for all two-phase alloys confirm the structures as fcc and L_{21}-ordered structure, respectively, in line with the XRD studies.

Martensite twins are observed in alloy $x = 3$ along with the presence of γ-phase (Figure 5(a)). The triple junction of γ-phase and martensite is shown in Figure 5(a) which accommodates different martensite morphologies. The triple-junction phase interface could act as the nucleating agent for martensite phase to nucleate and grow by providing the high energy defect density, are termed as the potent nucleation sites.[16] The martensitic nucleation is a heterogeneous process and arises due to the interactions between lattice defects such as dislocations, stacking faults in the parent phase with the strain fields in the microstructure. The interactions at grain boundaries and phase interfaces also act as catalytic reagent for the nucleation of martensite. The corresponding diffraction pattern of martensite shows the structural modulation with the appearance of the weak and periodic spots with regular interval around the main diffraction spot. The structural modulation is analyzed to be 10 M-modulated structure (Figure 5(b)) with the observation of 5 + 5 periodic lattice planes on either side of the Bragg diffracted spots. The appearance of periodic spots represents the sinusoidal modulation of lattice distortion due to the cooperative movement of atoms, and the lattice continuity is maintained. Similar modulated structures in Ni_2FeGa Heusler alloys are observed in TEM and discussed elsewhere.[6,7] 14 M-modulated martensite structure is also observed in alloy $y = 3$ shown in Figure 5(d) and the brightfield images of martensite plates are shown in Figure 5(c). The appearance of six periodic spots between two Bragg reflections is due to 14 M-modulated martensite structure.

C. *Magnetic Properties and Martensite Transformation*

The magnetic properties of Ni-Fe-Ga alloys are measured at room temperature and shown in Figure 6. The magnetic properties of Heusler alloys are affected by their super lattice structures. More commonly, Heusler phase is generalized to the stoichiometry of X_2YZ and they form L_{21}-ordered structure. X-atoms form two sublattices by occupying the tetrahedral positions at 8c (1/4,1/4,1/4). Y and Z atoms form two different sublattices by occupying the octahedral voids at 4a(0,0,0) and 4b (1/2,1/2,1/2), respectively. The

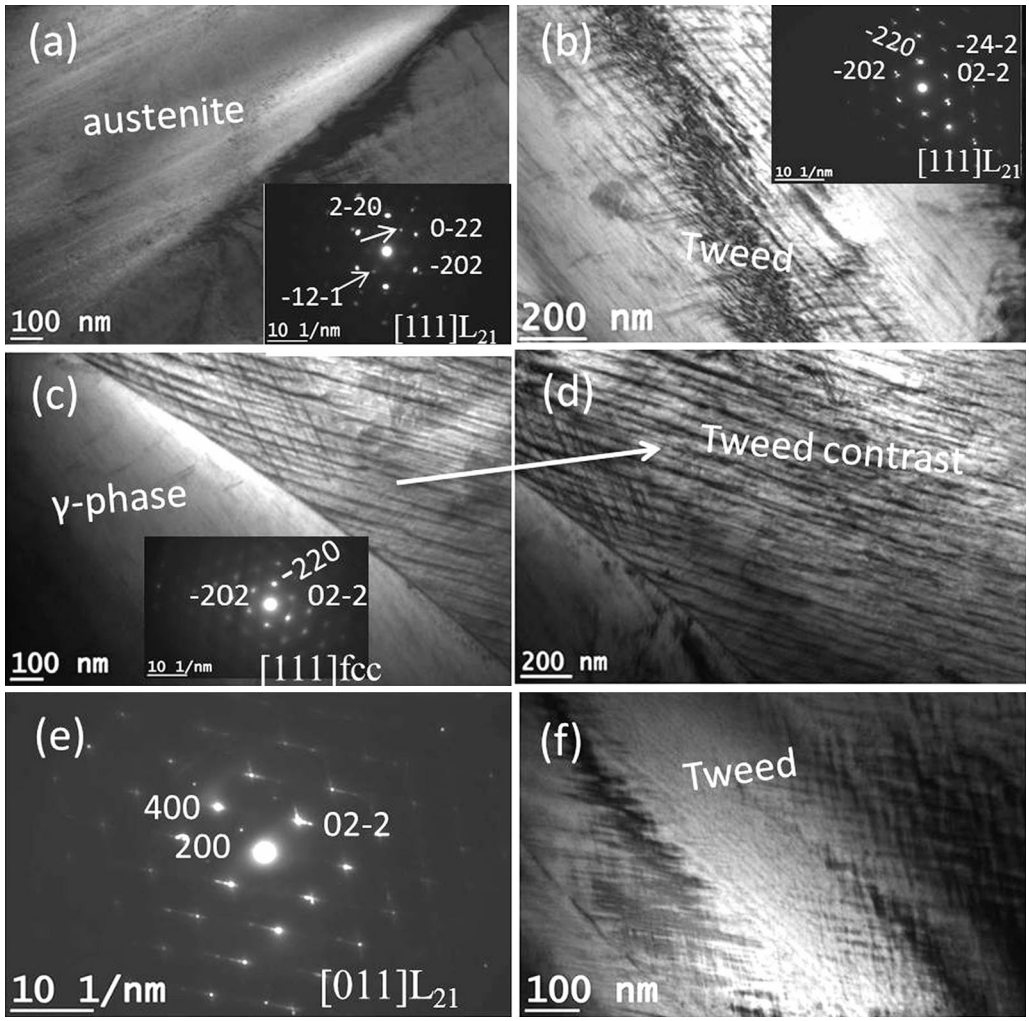

Fig. 4—(*a*) TEM bf-image of Ni-Fe-Ga Heusler alloy $z = 0$ and the corresponding diffraction pattern with diffuse spots and super lattice reflections of L_{21}-ordered structure (inset, a), (*b*) TEM bf-image of tweeds in alloy $z = 1$ and diffraction pattern of the corresponding tweed contrast (inset, b) shows the streaks emanating from Bragg diffracted spots, (*c*) TEM bf-images of alloy $x = 1$ show tweeds, and γ-phase are separated by phase interface, (inset, c) diffraction pattern of γ-phase, (*d*) tweed pattern zoomed from image (c), (*e*) Diffuse spots and super lattice reflections taken from (*f*) the tweed pattern of alloy $x = 2$.

interactions between the four interpenetrating fcc sublattices occupied by respective X, Y and Z atoms give rise to the net magnetic moment. The detail sublattice models and the magnetic interaction in Heusler alloys can be found elsewhere.[17–19] Importantly, X-atoms decide the lattice constant and Z-atoms mediate the Y–Y covalent interaction by providing p-d hybrid orbitals. In this article, the studied Ni_2FeGa Heusler alloys are all ferromagnetic in nature. In Ni-Fe-Ga Heusler alloys, mostly Fe-atoms contribute to the magnetic properties.[19,20] Magnetic properties are improved with Fe content in x and z alloy series. In the case of alloy series "y" with constant Fe content, magnetization value decreases as Ni replaces Ga. Phase-transformation behavior was studied using DSC (Figure 7). Alloy $y = 3$ has highest martensite transformation temperature with lowest Ga content (25 at. pct) and alloy $z = 0$ has lowest martensite transformation temperature with highest Ga content (29 at. pct).

In the case of alloys of x and y series, martensite transformation temperature increases, and magnetization decreases with the increasing x and y (Ni increases), whether Ni replaces Fe or Ga. For alloys of z-series with constant Ni content of 52 at. pct, as z increases (Fe increases), both the magnetization and the martensite transformation temperatures increase. Comparing the alloys of x and z series, in both cases, magnetization increases with increasing Fe content. Martensite transformation temperature increases with Ni-content at constant Ga (x-series) and as Ga content decreases (z-series) (Figure 8). That may be attributed to the role of Ga which stabilizes austenite phase in alloys of z-series and lowers the transformation temperature. For alloys of y-series with constant Fe content as Ni substitutes for Ga, martensite transformation temperature increases (as Ga content decreases) and lowers the magnetization value. In y and z alloy series, martensite transformation temperature increases due to the lower content of austenite stabilizing element Ga. In the case

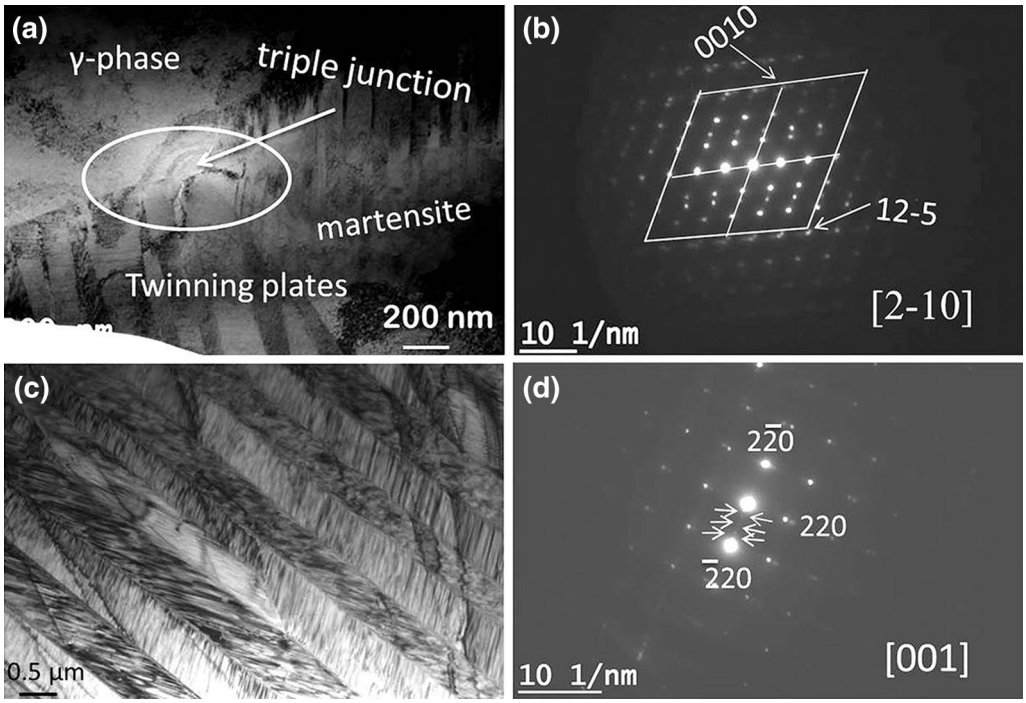

Fig. 5—TEM bf-images of Ni-Fe-Ga Heusler alloy $x = 3$ show (*a*) martensite twins and triple-phase boundary, (*b*) SAED pattern of 10 M-modulated martensite structure, (*c*) TEM bf-images of alloy $y = 3$ show stacking of martensite plates, (*d*) SAED pattern of 14 M-modulated martensite structure.

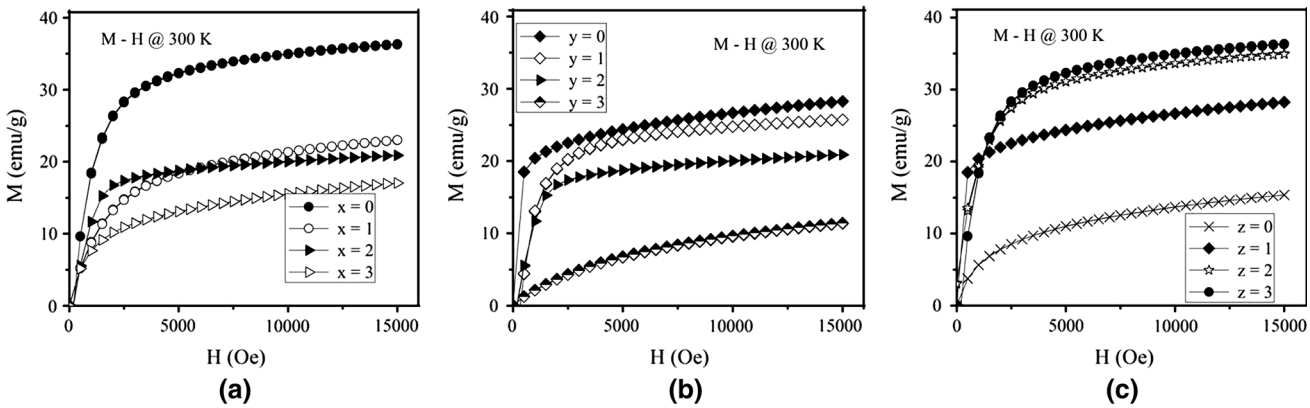

Fig. 6—Room-temperature [at 300 K (27 °C)] isothermal magnetic properties of (*a*) $Ni_{52+x}Fe_{22-x}Ga_{26}$, (*b*) $Ni_{52+y}Fe_{20}Ga_{28-y}$, (*c*) $Ni_{52}Fe_{19+z}Ga_{29-z}$ Heusler alloys.

of *x*-series alloys, with constant Ga content as Ni replaces Fe, by lowering the magnetic contribution, martensite phase gets stabilized. As the alloy composition changes, *e*/*a* ratio of the alloy also changes which influences both magnetic properties and martensite transformation behavior by modifying the free electron concentration.[21] *e*/*a* ratio represents the ratio of valence electrons to the number of atoms in the stoichiometry of the corresponding Heusler alloy. In the case of alloy series *x* and *y*, as *e*/*a* ratio increases, magnetization value decreases, and martensite transformation temperature increases (Figure 8). However, in *z* series alloy, as *e*/*a* ratio increases both magnetization and martensite transformation temperature increases. Mostly it dictates the role of Ni and Fe in the alloy composition as they provide large number of free electrons.

IV. DISCUSSION

The observation of different morphologies and modulated structures of martensite in Ni-Fe-Ga alloys is a step ahead toward possible shape memory applications of this kind of alloys. Due to low symmetry structure of martensite, it is possible to form different variants of martensites together in order to accommodate the transformation strain which results in various morphologies of martensite. During growth process, these

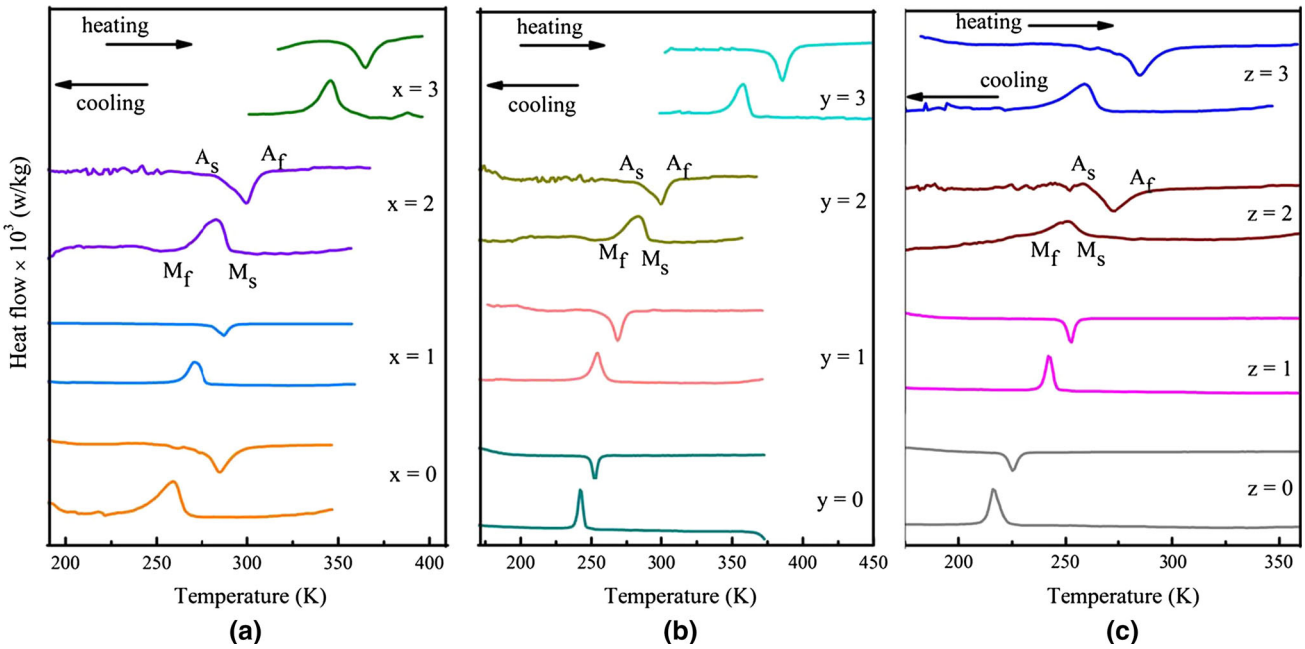

Fig. 7—Thermal analysis DSC curves of martensite transformation in (*a*) $Ni_{52+x}Fe_{22-x}Ga_{26}$, (*b*) $Ni_{52+y}Fe_{20}Ga_{28-y}$, (*c*) $Ni_{52}Fe_{19+z}Ga_{29-z}$ Heusler alloys.

variants interact with each other and present a composite microstructure. Martensite transformation occurs by typical first-order phase transition which is accomplished by nucleation and growth process by forming a new interface at the phase boundary and propagation of the interface. Once martensite nucleates at the γ-phase interface, it maintains the orientation relationship with the parent phase to minimize the strain energy. The structure and surface energy of the interface and the transformational strain energy affect the morphology and kinetics of the newly formed phase.[22] These types of martensite morphologies are formed by the accommodation process during the propagation of interface. The interface moves so as to consume the transformation strain in compatible with the other phase which also affects the structural modulation of newly formed martensite.

Modulated crystallography of martensite plays an important role to form different twin variants and enhances the accommodation process resulting in reduced stress requirement to move the twin boundaries. Again it is supported by the magnetic nature of Heusler alloys. Magnetocrystalline anisotropic property provides the required magnetostress for the movement of twin boundaries. The stress requirement for the twin boundary reorientation in magnetic field reduces drastically from nonmodulated martensite to modulated martensite.[23] Thus, the observation of 10- and 14 M-modulated martensite structures in Ni-Fe-Ga Heusler alloy $x = 3$ and alloy $y = 3$ supports the existing literatures and presents a good material for further shape memory studies.

The martensite phase in Heusler alloys gets stabilized by including the magnetic contribution to the total free energy change during martensite transformation. The magnetic saturation values and magnetic anisotropic properties of modulated martensite phase are higher than that of austenite phase in Heusler alloys.[24,25] The critical stress required for the twin boundary movement in modulated martensite structure is quite low and easily provided by the magnetic stress generated in the martensite phase due to high magneto crystalline anisotropic properties. Thus, the combination of modulated martesnite structure with high magnetic properties enables the material to experience large amount of recoverable magnetic strain in an external magnetic field which is highly desirable in magnetic shape memory applications. Structural phase transition in Heusler alloys is driven by strong electron–phonon coupling which modifies the density of states at Fermi level and creates instability toward phase transformation as temperature lowers. Thus, alloy composition plays an important role in this transition as it provides the number of free electrons, restructures the density of states and also modifies the magnetic properties. The effects of alloy composition on magnetic properties and phase-transformation behavior in Ni-Fe-Ga Heusler alloy have been discussed in this article. The presence of Fe improves the magnetic properties and stabilizes the γ-phase. Ga stabilizes the austenite phase in the microstructure. Hence, the role of Ga is to lower the transformation temperature and Ni raises the transition temperature. Fe plays a dual role. When Fe replaces Ga, both magnetic properties and martensite transformation temperature increases. However, when Fe replaces Ni, though it improves magnetization, martensite transformation temperature decreases. Hence, this investigation would be useful in designing the alloy for specific application.

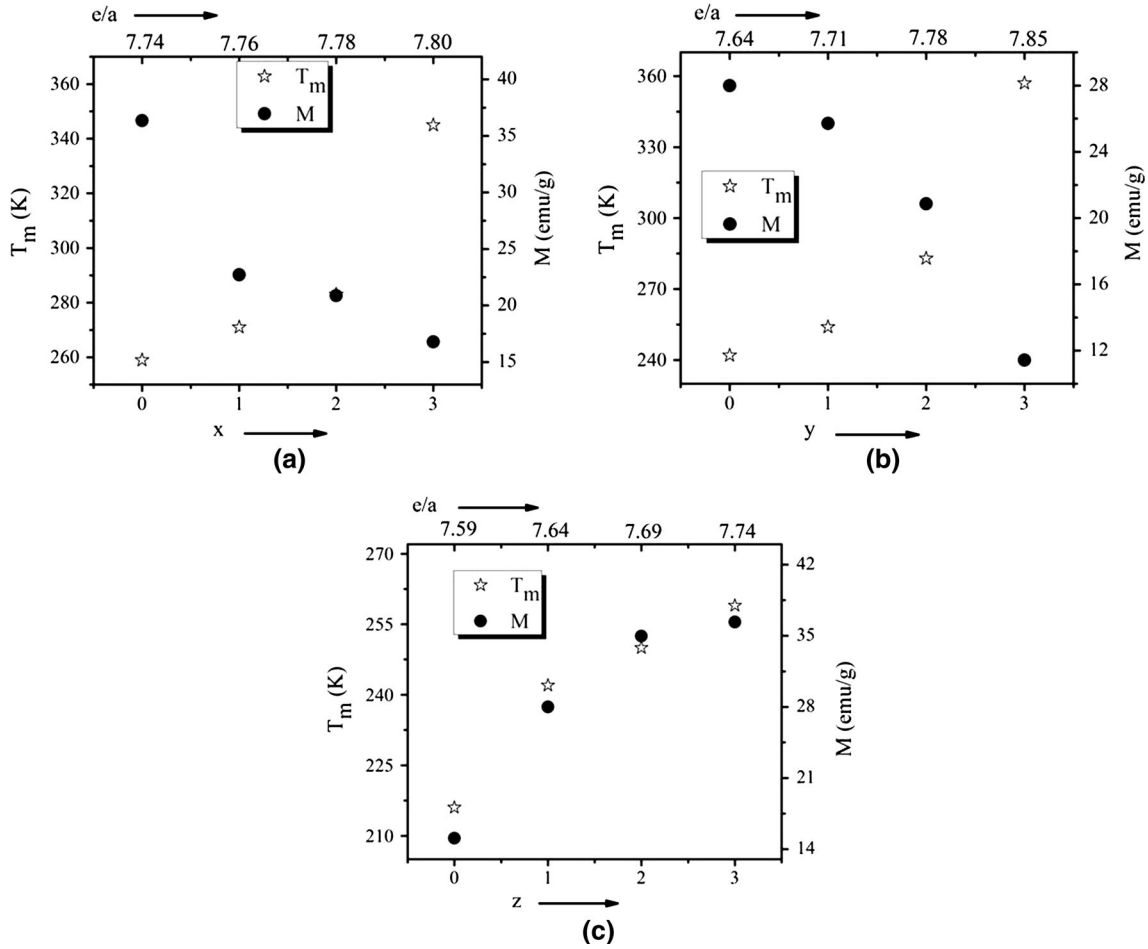

Fig. 8—Schematic representation of magnetic properties and martensite transformation behavior in (*a*) $Ni_{52+x}Fe_{22-x}Ga_{26}$, (*b*) $Ni_{52+y}Fe_{20}Ga_{28-y}$, (*c*) $Ni_{52}Fe_{19+z}Ga_{29-z}$ Heusler alloys. (Note: *e*/*a* ratio represents the ratio of valence electrons to the number of atoms in the stoichiometry of the corresponding Heusler alloy, T_m (martensite transformation temperature), *M* (magnetization)).

V. CONCLUSIONS

The martensite phase transformation and magnetic properties in Ni-Fe-Ga Heusler alloys are discussed with nine different alloy compositions. Alloy composition, phases present in the microstructure, magnetic properties, and martensite transformation are interconnected with each other in Ni-Fe-Ga Heusler alloys. This aspect of interdependency has been investigated by choosing alloy compositions around Heusler stoichiometry. The γ-phase formation could be suppressed with higher Ga-content in the alloy as it stabilizes austenite phase, but lowers the martensite transformation temperature. As Fe replaces Ga with constant Ni content, magnetic properties improve, and martensite transformation temperature also increases. This was attributed to the important role of Fe and Ga contents in the design of alloy composition. In the case of alloys where Ni substitutes either Fe or Ga, martensite transformation temperature increases, and magnetization value decreases.

ACKNOWLEDGMENTS

The authors wish to thank Mrs. D. Kanchanmala for TEM, Dr. Rama for DSC, and Mr. Muthukumaran for VSM measurement. Thanks are also due to SAIF, IIT-Madras for providing their facility to conduct DSC and VSM studies.

REFERENCES

1. H. Zheng, D. Wu, S. Xue, J. Frenzel, G. Eggeler, and Q. Zhai: *Acta Mater.*, 2011, vol. 59, pp. 5692–99.
2. J. Liu, T. Gottschall, K.P. Skokov, J.D. Moore, and O. Gutfleisch: *Nat. Mater.*, 2012, vol. 11, pp. 620–26.
3. R. Sahoo, A.K. Nayak, K.G. Suresh, and A.K. Nigam: *J. Magn. Magn. Mater.*, 2012, vol. 324, pp. 1267–71.
4. A. Biswas, G. Singh, S. Sarkar, M. Krishnan, and U. Ramamurty: *Intermetallics*, 2014, vol. 54, pp. 69–78.
5. J.F. Qian, H.G. Zhang, J.L. Chen, W.H. Wang, and G.H. Wu: *J. Cryst. Growth*, 2014, vol. 388, pp. 107–11.
6. J.B. Lu, H.X. Yang, H.F. Tian, L.J. Zeng, C. Ma, L. Feng, G.H. Wu, J.Q. Li, and J. Jansen: *J. Solid State Chem.*, 2010, vol. 183, pp. 425–30.

7. H.R. Zhang, C. Ma, H.F. Tian, G.H. Wu, and J.Q. Li: *Phys. Rev. B*, 2008, vol. 77, p. 214106(1–12).
8. Q.H. Liu, J. Liu, Y.J. Huang, Q.D. Hu, and J.G. Li: *J. Alloys Compd.*, 2013, vol. 571, pp. 186–91.
9. H. Sehitoglu, J. Wang, and H.J. Maier: *Int. J. Plast.*, 2012, vol. 39, pp. 61–74.
10. Y.J. Huang, Q.D. Hu, N. Bruno, I. Karaman, and J.G. Li: *Mater. Lett.*, 2014, vol. 114, pp. 11–14.
11. J.I. Perez-Landazabal, V. Recarte, V. Sanchez-Alarcos, J.A.R. Velamazan, M.J. Ruiz, P. Link, E. Cesari, and Y.I. Chumlyakov: *Phys. Rev. B.*, 2009, vol. 80, p. 144301(1–6).
12. H. Nath and G. Phanikumar: *Mater. Sci. Forum*, 2014, vols. 790–791, pp. 199–204.
13. Y. Li, C. Jiang, T. Liang, Y. Ma, and H. Xu: *Scripta Mater.*, 2003, vol. 48, pp. 1255–58.
14. V.K. Sharma, M.K. Chattopadhyaya, R. Kumar, T. Ganguli, R. Kaul, S. Majumdar, and S.B. Roy: *J. Phys. D Appl. Phys.*, 2007, vol. 40, pp. 3292–99.
15. M. Umemoto, E. Yoshitake, and I. Tamura: *J. Mater. Sci.*, 1983, vol. 18, pp. 2893–2904.
16. R.V.S. Prasad, M. Srinivas, M. Raja, and G. Phanikumar: *Metall. Trans. A*, 2014, vol. 45A, pp. 2161–70.
17. T. Graf, F. Casper, J. Winterlik, B. Balke, G.H. Fecher, and C. Felser: *Z. Anorg. Allg. Chem.*, 2009, vol. 635, pp. 976–81.
18. J. Kubler, A.R. Williams, and C.B. Sommers: *Phys. Rev. B.*, 1983, vol. 28, pp. 1745–55.
19. M.B. Sahariah, S. Ghosh, C.S. Singh, S. Gowtham, and R. Pandey: *J. Phys. Conds. Matter*, 2013, vol. 25, p. 025502(1–7).
20. Z.H. Liu, H.N. Hu, G.D. Liu, Y.T. Cui, M. Zhang, J.L. Chen, and G.H. Wu: *Phys. Rev. B*, 2004, vol. 69, p. 134415(1–6).
21. R.V.S. Prasad, M. Raja, and G. Phanikumar: *Intermetallics*, 2012, vol. 25, pp. 42–47.
22. Y. Ji, Z. Liu, and H. Ren: *Adv. Mater. Res.*, 2011, vols. 201–203, pp. 1612–18.
23. Y. Sutou, N. Kamiya, T. Omari, R. Kainuma, K. Ishida, and K. Oikawa: *Appl. Phys. Lett.*, 2004, vol. 84, pp. 1275–77.
24. A. Sozinov, A.A. Likhachev, N. Lanska, and K. Ullakko: *Appl. Phys. Lett.*, 2002, vol. 80, pp. 1746–48.
25. L. Straka and O. Heczko: *J. Appl. Phys.*, 2003, vol. 93, pp. 8636–38.